Available online at www.sciencedirect.com

SciVerse ScienceDirect

Ceramics International 38 (2012) 3807–3813

CERAMICS INTERNATIONAL

www.elsevier.com/locate/ceramint

Rapid synthesis of low thermal expansion materials of $Ca_{1-x}Sr_xZr_4P_6O_{24}$

D.Y. Xie, Z.H. Wang, X.S. Liu, W.B. Song, B.H. Yuan, E.J. Liang *

School of Physical Science & Engineering and Key Laboratory of Materials Physics of Ministry of Education of China, Zhengzhou University, Zhengzhou 450052, China

Received 4 June 2011; received in revised form 7 January 2012; accepted 12 January 2012
Available online 1 February 2012

Abstract

A rapid synthesis method is introduced for the synthesis of low thermal expansion materials of $Ca_{1-x}Sr_xZr_4P_6O_{24}$ ($x = 0$, 0.5 and 1) and optimum synthesizing conditions are obtained. It is shown that these materials can be synthesized by one-step sintering by putting the preheated mixture of $CaCO_3$, $SrCO_3$ and $NH_4H_2PO_4$ directly into a pipe furnace at the sintering temperature (1673–1873 K). With this method, the sintering procedure is much simplified and sintering time and energy exhausts are considerably reduced with respect to the conventional solid state reactions which usually require multiple-step and longer time sintering at different temperatures with intermediate grindings for the synthesis of these materials. By putting the samples directly at the sintering temperature, the formation of the secondary phase ZrP_2O_7 can be largely avoided. This insures the rapid synthesis of $Ca_{1-x}Sr_xZr_4P_6O_{24}$. MgO is introduced to increase the density of $Ca_{0.5}Sr_{0.5}Zr_4P_6O_{24}$ ceramics. A sintered density of 3.10 g cm^{-3}, relative density of 96.2% for $Ca_{0.5}Sr_{0.5}Zr_4P_6O_{24}$ is obtained with 1.0 wt.% MgO. The coefficients of thermal expansion are about 0.27×10^{-6} K^{-1}. Raman spectroscopic and differential scanning calorimetry (DSC) analyses reveal that there are no phase transitions of all the samples from 113 K to 1423 K.

Keywords: Ceramics sintering; Low thermal expansion material; Alkaline earth zirconium phosphate; Density; Raman spectroscopy; DSC

1. Introduction

The structural family of low-expansion materials derived from the prototype composition $NaZr_2(PO_4)_3$ (NZP) has received great interest for their wide applications such as fast ionic conductors, devices requiring good thermal shock resistance and catalyst supports in automobiles, etc. [1–8]. The crystal structure of NZP consists of corner-sharing PO_4 tetrahedra and ZrO_6 octahedra, building up a flexible and stable three-dimensional network [9]. The network has stable hexagonal lattice with structural holes that can be partially or fully occupied by calcium, strontium, sodium or other substituting ion(s). Due to its flexibility to accommodate almost the whole periodic table, NZP structure has proved to be an excellent host to immobilize almost all 42 elements present in commercial nuclear waste and still maintains its structural integrity [10,11]. Extremely wide variations of cation compositions with the conservation of crystallographic characteristics close to those of NZP permit to create new materials with desired properties [3]. An important property of the NZP family of materials is low thermal expansion, which can be controlled and tailored by ionic substitutions. The low thermal expansion behavior of these materials is due to the rotation of polyhedral network and the coupling between octahedra and tetrahedra [7,12].

Limaye et al. [13] studied the thermal expansion properties of $CaZr_4P_6O_{24}$ and found that the axial thermal expansion of $CaZr_4P_6O_{24}$ was negative along the *a* axis and positive along the *c* axis between room temperature and 773 K while $SrZr_4P_6O_{24}$ and $BaZr_4P_6O_{24}$ exhibited the opposite behavior. By taking these properties, a single phase, crystalline solid solution of $Ca_{1-x}M_xZr_4P_6O_{24}$ (M = Sr or Ba) with near zero bulk thermal expansion and very low anisotropy were realized. This is due to bond angle distortions brought about by the coupled rotation of the corner-shared PO_4 and ZrO_6 polyhedra under thermal stresses [14,15]. The structure of NZP compound in most cases belongs to the R-3c group whereas structure of $CaZr_4P_6O_{24}$, Sr and Ba modified $CaZr_4P_6O_{24}$ fits into R-3 [15,16].

A literature search shows that the synthesis of $Ca_{1-x}Sr_xZr_4P_6O_{24}$ materials is quite a hard task [15–19]. They were prepared by either solid state reaction method or a sol–gel

* Corresponding author. Tel.: +86 371 67767838; fax: +86 371 67766629.
E-mail address: ejliang@zzu.edu.cn (E.J. Liang).

0272-8842/$36.00
doi:10.1016/j.ceramint.2012.01.029

route. The traditional methods for synthesizing these compounds are quite tedious and time and energy exhaustive. For example, the sintering of $CaZr_4P_6O_{24}$, $SrZr_4P_6O_{24}$ and $Ca_{1-x}Sr_xZr_4P_6O_{24}$ requires respectively 48 and 48–72 h at 1473 K by solid state reactions in addition to several pre-calcination steps at different temperatures with intermediate grindings [17,18]. Chakraborty et al. [19] synthesized $Ca_{1-x}Sr_xZr_4P_6O_{24}$ by fusing the powder mixtures at 473 K for 15 h and calcining at 873 K for 4 h, then firing once again at 1173 K for 16 h and finally sintering at 1573 K for 6 h, and showed that the samples contained 7–10 wt.% secondary phase ZrP_2O_7.

At the same time, the samples prepared by solid state reactions have low densities (73–81.3%) [17]. In order to improve the sintering density, Yoon [20] chose Li_2O as a sintering aid through pressureless liquid phase sintering. The sintered density of $CaZr_4(PO_4)_6$ reached 2.95 g cm^{-3} at 92% of the theoretical density. ZnO was also used to prompt sintering [18,19]. However, introduction of ZnO resulted in the formation of $Zn_3(PO_4)_2$ and free ZrO_2 which was evident in the microstructure as white precipitate [19]. Due to formation of the high expansion $Zn_3(PO_4)_2$ phase and free ZrO_2 during sintering, all the compounds with ZnO addition exhibited higher coefficients of thermal expansion. Besides, the microstructure of all the samples shows pores and an irregular micro-crack network.

The sol–gel method has the advantage of obtaining nanoparticles which are preferred for realizing high density samples. However, it requires tedious preparing procedures of the sol–gels, long time drying (24 h at 338 K) and calcinations (at 973 K–1473 K for 16–24 h). Besides, the solution method requires also expensive chemicals such as $ZrOCl_2{\cdot}8H_2O$ and large amount of chemicals other than the starting materials. $ZrOCl_2{\cdot}8H_2O$ is poor in stability in air. Exploring new synthetic procedures for this class of materials are certainly needed.

In this paper, we report on the rapid synthesis of this family of materials aiming at simplifying the sintering procedures and exploring a time and energy saving method. It is shown that $Ca_{1-x}Sr_xZr_4P_6O_{24}$ ($x = 0$, 0.5 and 1) can be successfully synthesized by one-step high temperature solid state reactions. With this method, time and energy consumptions are greatly reduced with respect to the conventional methods. By adding proper amount of MgO, the sintered density of the samples can be much improved, reached 3.10 g cm^{-3}, 96% of the theoretical density. Besides, we also present the first Raman spectroscopic study on $Ca_{1-x}Sr_xZr_4P_6O_{24}$ materials. From our temperature-dependent Raman spectroscopy and differential scanning calorimetry (DSC) analyses, it is concluded that these materials are stable at least from 113 K to about 1400 K.

2. Experimental procedure

2.1. Sample preparation

The $Ca_{1-x}Sr_xZr_4P_6O_{24}$ ($x = 0$, 0.5 and 1) samples were synthesized by high-temperature solid state reactions. Commercial chemicals of CaO, $SrCO_3$, ZrO_2 and $NH_4H_2PO_4$ (99.9% purity) were mixed according to the stoichiometric ratios of destination materials of $CaZr_4P_6O_{24}$, $SrZr_4P_6O_{24}$ and $Ca_{0.5}Sr_{0.5}Zr_4P_6O_{24}$. The mixtures were ground in an agate mortar for 2 h, and then preheated at 873 K for 4 h to decompose $CaCO_3$, $SrCO_3$ and $NH_4H_2PO_4$ with emission of carbon dioxide, ammonia and water vapors. The powders were then manually pressed into pellets (φ1.5 cm and 0.2 mm thick) with a 10 MPa pressure. The green pellets were put directly into a pipe furnace which was preheated to sintering temperature (1600–1800 K). In order to search for optimum conditions for the synthesis of these materials, different combinations of sintering temperatures and time were explored for each compositional ratio. Detailed sintering temperature and time for each sample are given in Section 3.1.

2.2. Measurement and characterization

Each sample was analyzed by X-ray diffraction (XRD) with an X'Pert PRO X-ray Diffractometer and by Raman spectroscopy with a Renishaw MR-2000 Raman spectrometer. The densities of the samples were measured by using the Archimedes' principle. Microstructures of the samples were observed with JSM-6700F field emission scanning electron microscope. The DSC study was done on an Ulvac Sinku-Riko differential scanning calorimetry, Model 1500M/L in the temperature range of 300–1423 K, with the heating and cooling rates of 10 K min^{-1}. The coefficients of thermal expansion were measured with a Linseis L76PT Dilatometer.

3. Results and discussion

3.1. CSZP sintering characteristics

3.1.1. Sintering temperature and time

In order to search for the optimum sintering conditions for the synthesis of $CaZr_4P_6O_{24}$, $SrZr_4P_6O_{24}$ and $Ca_{0.5}Sr_{0.5}Zr_4P_6O_{24}$, the samples were put into a pipe furnace pre-heated to the sintering temperature and sintered at different temperatures and time. Fig. 1a–d shows the X-ray diffraction patterns of

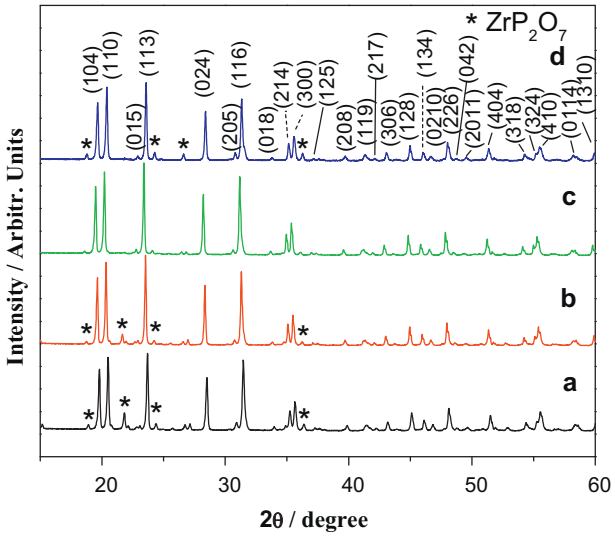

Fig. 1. The XRD patterns of $CaZr_4P_6O_{24}$ sintered at 1673 K for (a) 10 h, (b) 12 h, (c) 16 h and (d) 24 h, respectively.

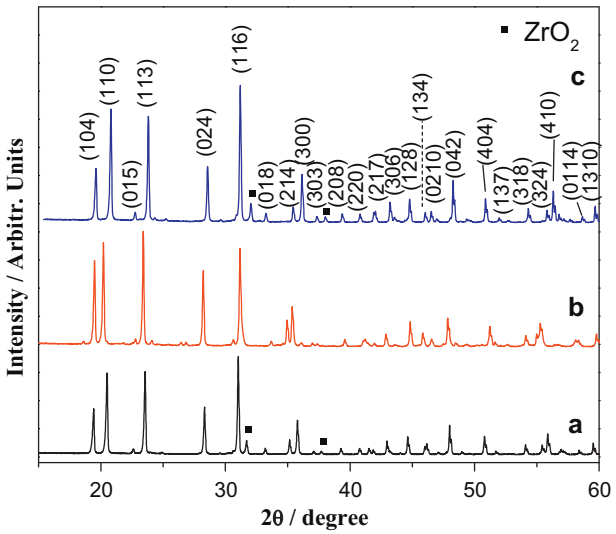

Fig. 2. The XRD patterns of $CaZr_4P_6O_{24}$ sintered at (a) 1573 K for 24 h, (b) 1673 K for 16 h and (c) 1773 K for 8 h, respectively.

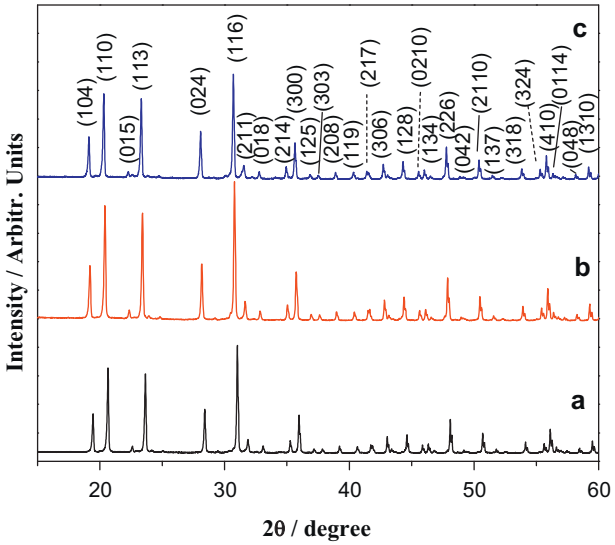

Fig. 4. The XRD patterns of $SrZr_4P_6O_{24}$ sintered at (a) 1573 K for 24 h, (b) 1673 K for 16 h and (c) 1773 K for 8 h, respectively.

$CaZr_4P_6O_{24}$ sintered at 1673 K for 10, 12, 16 and 24 h, respectively. It is shown that the samples sintered for 16 and 24 h are fully crystallized to form pure $CaZr_4P_6O_{24}$ while a little amount of secondary phases appear with less sintering time as indicated by the diffuse peaks at lower angles. The secondary phases are identified to be ZrO_2 (ICDD-JCPDS-PDF No. 00-024-1165) and ZrP_2O_7 (ICDD-JCPDS-PDF No. 01-075-0926). It is concluded that the optimal time is 16 h for the synthesis of $CaZr_4P_6O_{24}$ when it is sintered at 1673 K. However, when the samples were sintered at lower or higher temperatures, longer or shorter sintering time is required. It is found that it requires 24 h when sintered at 1573 K and only 8 h when sintered at 1773 K as shown in Fig. 2.

Fig. 3 shows the XRD patterns of $SrZr_4P_6O_{24}$ samples sintered at 1573 K for 10, 20, 24 and 48 h, respectively. It is shown that single phase specimens require at least 20 h sintering at this temperature. Otherwise, the secondary phases of ZrO_2 and ZrP_2O_7 exist. By increase the sintering temperature to 1673 K or 1773 K, the time could be shortened to 16 h or 8 h, respectively, as shown in Fig. 4.

Fig. 5 shows the XRD patterns of $Ca_{0.5}Sr_{0.5}Zr_4P_6O_{24}$ sintered at 1673 K for 12, 16, 20 and 24 h, respectively. It is clear that the secondary phase of ZrP_2O_7 appears in the sample sintered for 12 h and vanishes for longer sintering time. Optimum conditions for the synthesis of pure samples are explored. It is shown that when sintered at 1573 K, 1673 K, 1773 K and 1823 K, pure samples can be synthesized in 24, 16, 8 and 4 h, respectively, as shown in Fig. 6.

In contrast to traditional solid state reactions, all these samples are synthesized in one-step sintering without intermediate grindings. The sintering method presented here simplifies the synthesis procedures and saves energy and time

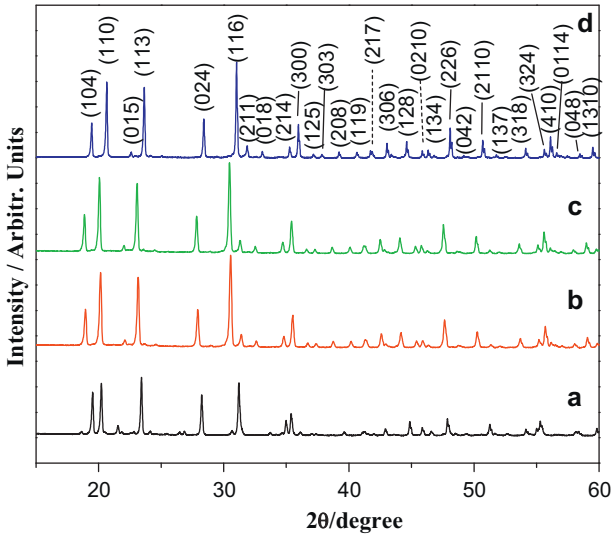

Fig. 3. The XRD patterns of $SrZr_4P_6O_{24}$ sintered at 1573 K for (a) 16 h, (b) 20 h, (c) 24 h and (d) 48 h, respectively.

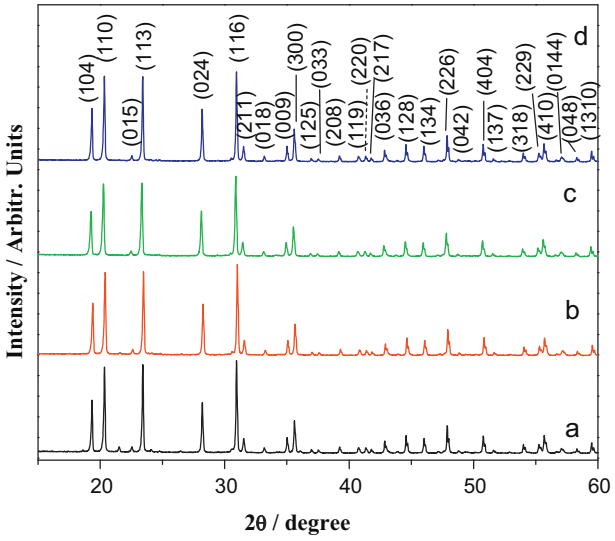

Fig. 5. The XRD patterns of $Ca_{0.5}Sr_{0.5}Zr_4P_6O_{24}$ sintered at 1673 K for (a) 12 h, (b) 16 h, (c) 20 h and (d) 24 h, respectively.

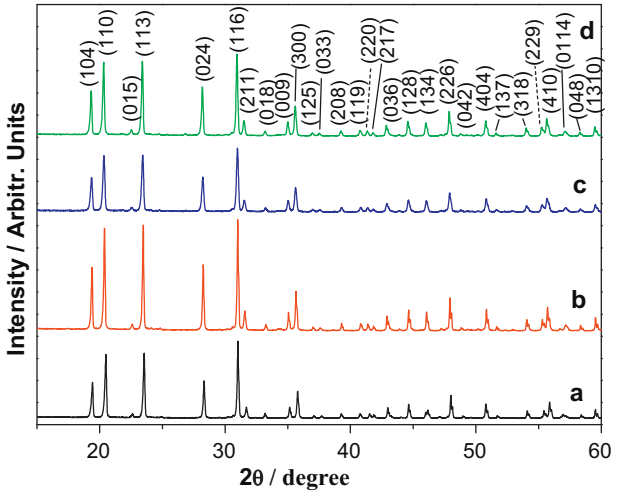

Fig. 6. The XRD patterns of $Ca_{0.5}Sr_{0.5}Zr_4P_6O_{24}$ sintered at (a) 1573 K for 24 h, (b) 1673 K for 16 h, (c) 1773 K for 8 h and (d) 1823 K for 4 h, respectively.

Table 1
Densities of $Ca_{0.5}Mg_{0.5}Zr_4(PO_4)_6$ sintered at different conditions.

MgO (%)	T (K)	t (h)	ρ (g cm^{-3})	d (%)
0	1673	16	2.1077	64.65
0	1773	8	2.3434	71.88
0	1823	4	2.4167	74.13
0.5	1673	16	2.6451	82.15
0.5	1773	8	2.6935	83.65
0.5	1823	4	2.6512	82.34
1.0	1673	16	2.7956	86.82
1.0	1773	8	3.0984	96.22
1.0	1823	4	2.8050	87.11
1.0	1773	7	2.8951	89.91
1.0	1773	7.5	2.9251	90.84
1.0	1773	8.5	3.0216	93.84
1.0	1773	9	2.9047	90.21
1.5	1673	16	2.8150	86.35
1.5	1773	8	2.9014	89.00
1.5	1823	4	2.3824	86.88

costs greatly. The energy consumption can be roughly estimated by $k_BT \times t$, where k_B is Boltzmann constant, T is the absolute temperature and t is the sintering time.

3.1.2. Sintering conditions on the ceramic body of $Ca_{0.5}Sr_{0.5}Zr_4P_6O_{24}$

The previously reported synthesis of $Ca_xMg_{1-x}Zr_4(PO_4)_6$ by solid state reactions required a large number of grinding, mixing, and heating steps and the sintered bodies had usually low density (65–80% of the theoretical density) [13,17]. Based on our studies described above, the synthesis procedure of the $Ca_{0.5}Mg_{0.5}Zr_4(PO_4)_6$ ceramic body may be simplified by one-step sintering. In order to increase the density of the ceramics, proper amount of MgO additive is introduced to improve the densification rate. Table 1 gives the densities of the $Ca_{0.5}Mg_{0.5}Zr_4(PO_4)_6$ ceramic bodies synthesized at different temperatures and sintering time with and without addition of MgO, respectively. It is shown that the relative density increases from about 64% to 74% of the theoretical density with sintering temperature from 1673 K to 1873 K without addition of MgO. However, the relative density can be much improved with addition of MgO. It increases to about 83% with 0.5 wt.% MgO, to 96% with 1.0 wt.% MgO and to 89% with 1.5 wt.% MgO. It seems that there exist an optimum sintering temperature and time with addition of MgO, being 1773 K and 8 h, respectively.

Fig. 7 shows the SEM micrographs of the fractured cross-sections of the $Ca_{0.5}Sr_{0.5}Zr_4P_6O_{24}$ sintered at 1773 K and 1823 K, respectively. It can be seen that the sample synthesized at 1773 K has much smaller grain size and fewer pores than that synthesized at 1823 K, resulting in a higher density of the former than the latter. It seems that there formed on the surface of crystallites small amount of the liquid phase which connected the crystallites together and preventing the growth of grains when the sample was sintered at 1773 K. However, when the sintering temperature is higher, a higher volume of liquid phase was formed, leading to the bubble expansion and hence lower sintering density, the so-called ''over sintering'' phenomenon. It can be inferred that when the sintering temperature is too low (lower than 1773 K), the amount of liquid phase formed is not sufficient to form densified bodies in which a lot of voids and pores exist, leading to very low sintering density, the so-called ''under firing'' phenomenon.

Table 1 indicates also that the sintering time has a great impact on the densification of the $Ca_{0.5}Sr_{0.5}Zr_4P_6O_{24}$ ceramics. For the samples sintered at 1773 K, the ceramic density essentially increases with sintering time till 8 h and decreases

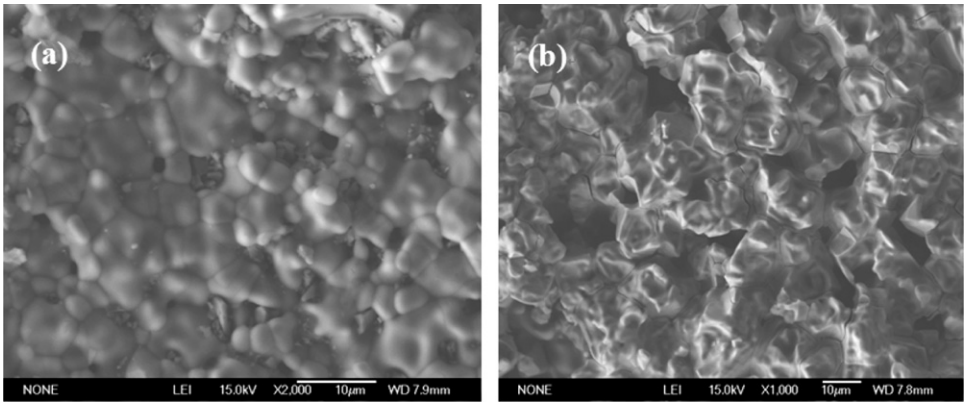

Fig. 7. SEM images of the fractured cross-sections of $Ca_{0.5}Sr_{0.5}Zr_4P_6O_{24}$ ceramics sintered at 1773 K for 8 h and 1823 K for 4 h, respectively.

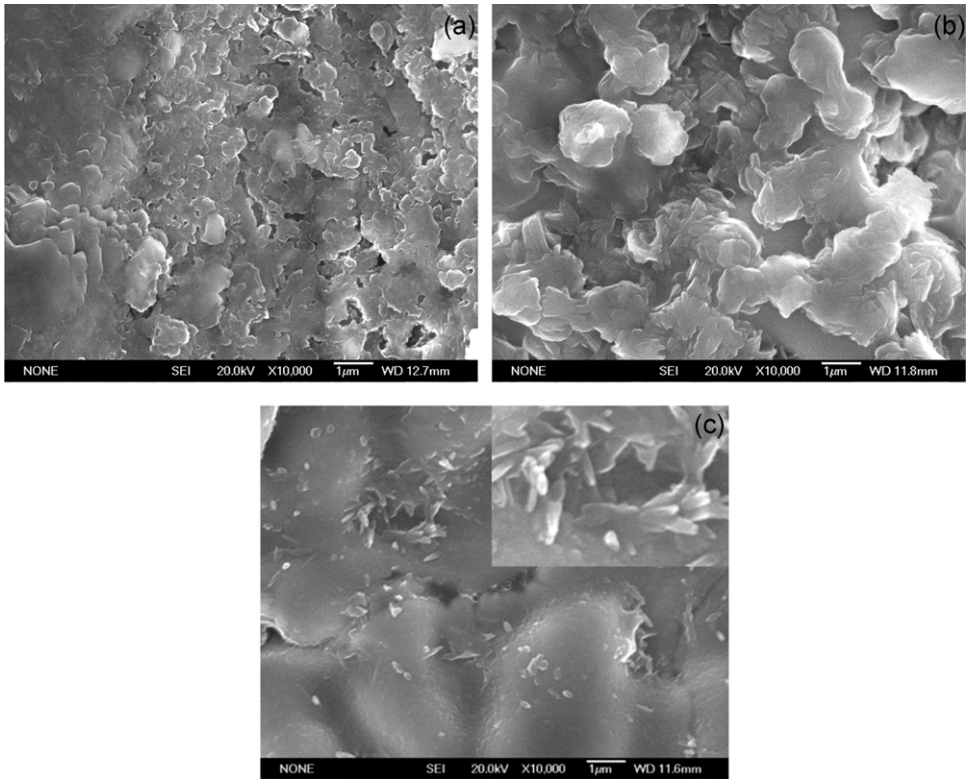

Fig. 8. SEM images of $Ca_{0.5}Sr_{0.5}Zr_4P_6O_{24}$ ceramics sintered at 1773 K for 8 h doped with (a) 0.5, (b) 1.0 and (c) 1.5 wt.% MgO, respectively.

when the sintering time lasted longer. This suggests that the density of ceramic body cannot be improved by extending the sintering time longer than 8 h at this temperature. At proper sintering temperature and time, the sintering additive forms enough glass phase in the boundary of grains, preventing further growth of the grain size and making the dispersed phase adhesive into the continuous phase. When the sintering time is longer, an excess volume of liquid phase will be formed and bubbles develop, leading to pores and hence lower density. It does not meet with the classical theory that usually the crystal grains do not grow rapidly at the end of sintering. When the sintering time is shorter, the amount of the liquid phase may be not sufficient for densification of the samples.

Fig. 8a–c exhibit the SEM images of $Ca_{0.5}Sr_{0.5}Zr_4P_6O_{24}$ ceramics with 0.5, 1.0 and 1.5 wt.% MgO sintered at 1773 K for 8 h, respectively. It is shown that there are numerous pores among grains for the sample with 0.5 wt.% MgO. When the content of MgO reaches 1.0 wt.%, the grains combine into larger-size granules with much fewer pores, causing the density of ceramics to increase. However, further increase in the content of MgO (to 1.5 wt.%) leads to a lot of nanorods sticking out of the larger-size granules, which may result in a lower density of ceramics.

3.2. Raman spectra and DSC analysis

Fig. 9 shows the Raman spectra of $CaZr_4P_6O_{24}$, $SrZr_4P_6O_{24}$ and $Ca_{0.5}Sr_{0.5}Zr_4P_6O_{24}$, respectively. The Raman spectra of these samples exhibit a common feature of the frame-work structures consisting of corner-sharing MO_4 (M = W, Mo, P) tetrahedra and AO_6 (A = Zr, Hf or trivalent cations) octahedra, displaying a wide phonon band gap between the stretching and bending modes. Different vibrational modes can therefore be easily identified. The Raman bands from 1100 to 950 cm^{-1}, from 550 to 650 cm^{-1}, and from 550 to 400 cm^{-1} can be identified as asymmetric and symmetric stretching vibrational modes ($\nu_1 + \nu_3$), asymmetric (ν_4) and symmetric bending (ν_2)

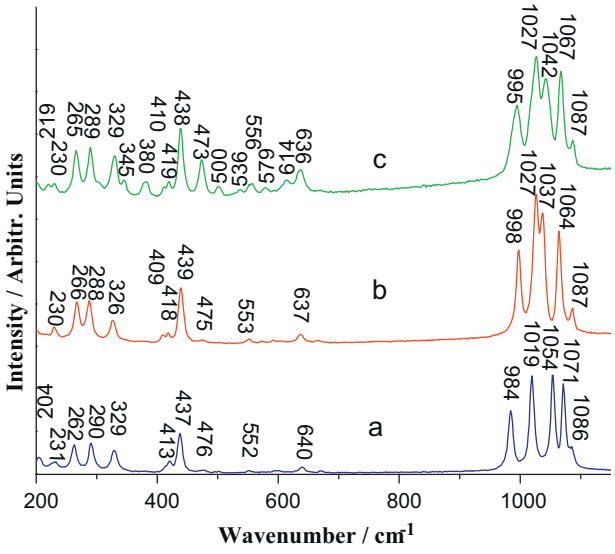

Fig. 9. Raman spectra of (a) $CaZr_4P_6O_{24}$, (b) $SrZr_4P_6O_{24}$, and (c) $Ca_{0.5}Sr_{0.5}Zr_4P_6O_{24}$.

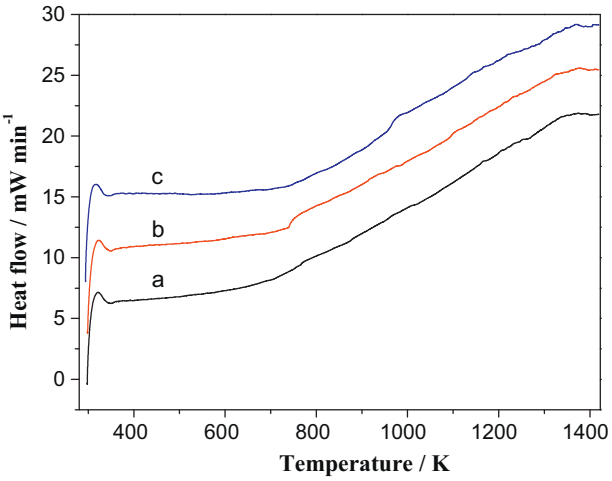

Fig. 10. Typical DSC scan for $Ca_{1-x}Sr_xZr_4P_6O_{24}$ (a) $x = 0$, (b) $x = 0.5$ and (c) $x = 1.0$.

modes in the PO_4^{3-} tetrahedra in $Ca_{1-x}Sr_xZr_4P_6O_{24}$, respectively, while those below 400 cm^{-1} can be attributed to the external modes, translational and librational motions of the polyhedra [21,22].

Although $CaZr_4P_6O_{24}$, $SrZr_4P_6O_{24}$ and $Ca_{0.5}Sr_{0.5}Zr_4P_6O_{24}$ exhibit similar phonon band structures due to structural similarity, the Raman band positions are obviously affected by Ca^{2+} or Sr^{2+} cations as shown by the stretching modes in spectra *a* and *b* of Fig. 9. It is shown that the Raman spectrum of $Ca_{0.5}Sr_{0.5}Zr_4P_6O_{24}$ resembles more to $SrZr_4P_6O_{24}$ than to $CaZr_4P_6O_{24}$, indicating Sr^{2+} has a larger influence in the P–O vibrations than Ca^{2+}.

Temperature dependence of the Raman spectra between 113 K and 823 K shows that there are no distinct changes in the Raman spectra except the red shifts of the band positions, suggesting no phase transitions occurring in this temperature range. Fig. 10 shows DSC scans of the samples. No endothermic or exothermic peaks appear form room temperature to 1423 K. Considering the Raman results, these samples maintain their structure at least from 113 K to 1423 K.

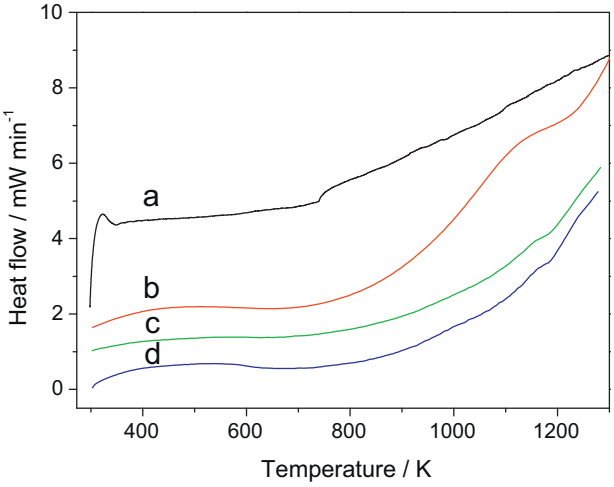

Fig. 11. Typical DSC scan for $Ca_{0.5}Sr_{0.5}Zr_4P_6O_{24}$ sintered at 1773 K for 8 h without (a) and with (b) 0.5, (c) 1.0 and (d) 1.5 wt.% MgO, respectively.

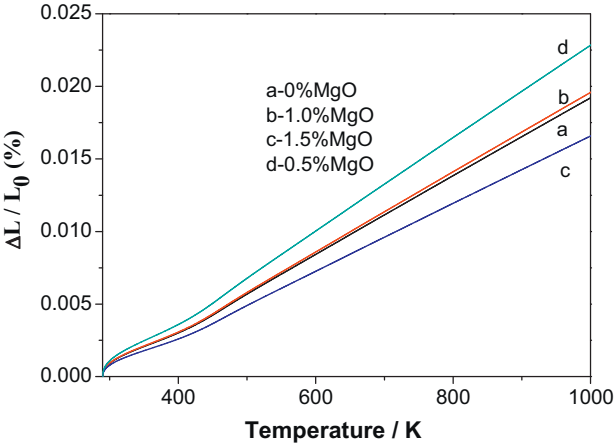

Fig. 12. Relative length changes of $Ca_{0.5}Sr_{0.5}Zr_4P_6O_{24}$ without and with 0.5, 1.0 and 1.5 wt.% MgO sintered at 1773 K for 8 h, respectively.

Fig. 11a–d present the DSC scans of the samples sintered at 1773 K for 8 h without and with 0.5, 1.0 and 1.5 wt.% MgO, respectively. It is found that no obvious endothermic or exothermic peaks are observed, which indicates that the samples are stable and without phase transition after adding MgO with 0.5, 1.0 and 1.5 wt.%.

Fig. 12 shows the relative length changes of the $Ca_{0.5}Sr_{0.5}Zr_4P_6O_{24}$ synthesized at 1773 K for 8 h without and with 0.5, 1.0 and 1.5% MgO, respectively. It is shown that the addition of MgO has little effect on its thermal expansion property of the $Ca_{0.5}Sr_{0.5}Zr_4P_6O_{24}$. The coefficients of thermal expansion are about $0.26 \times 10^{-6}\,K^{-1}$, $0.31 \times 10^{-6}\,K^{-1}$, $0.27 \times 10^{-6}\,K^{-1}$ and $0.22 \times 10^{-6}\,K^{-1}$ for the undoped and 0.5, 1.0 and 1.5 wt.% MgO-doped samples, respectively, indicating a low positive thermal expansion character of $Ca_{0.5}Sr_{0.5}Zr_4P_6O_{24}$.

4. Conclusions

The materials of $Ca_{1-x}Sr_xZr_4P_6O_{24}$ ($x = 0$, 0.5 and 1.0) have been synthesized by solid state reactions and optimum sintering conditions have been explored. The optimal conditions for the preparation of Ca_{1-x} $Sr_xZr_4P_6O_{24}$ are 1673 K for 16 h ($x = 0$), 1773 K for 8 h ($x = 0.5$) and 1773 K for 10 h ($x = 1.0$), respectively. Raman spectroscopic and DSC analyses indicate that there are no structure changes between 113 K and 1423 K. MgO was introduced to improve the sintering ability of the ceramics of $Ca_{0.5}Sr_{0.5}Zr_4P_6O_{24}$. It is shown that the density of the ceramics can be greatly improved by adding 1.0 wt.% MgO and sintering at 1773 K. The coefficients of thermal expansion are about $0.26 \times 10^{-6}\,K^{-1}$, $0.31 \times 10^{-6}\,K^{-1}$, $0.27 \times 10^{-6}\,K^{-1}$ and $0.22 \times 10^{-6}\,K^{-1}$ for the undoped and 0.5, 1.0 and 1.5 wt.% MgO-doped samples, respectively.

Acknowledgement

This work was supported by the National Science Foundation of China (No. 10974183).

References

[1] J. Alamo, R. Roy, Crystal chemistry of the $NaZr_2P_3O_{12}$, NZP or CTP structure family, J. Mater. Sci. 21 (1986) 444–450.

[2] V.I. Petkov, A.I. Orlova, G.N. Kazantsev, S.G. Samoilov, M.L. Spiridonova, Thermal expansion in the Zr and 1-, 2-valent complex phosphates of $NaZr_2(PO_4)_3$ (NZP) structure, J. Therm. Anal. Calorim. 66 (2001) 623–632.

[3] V.I. Petkov, A.I. Orlova, Crystal-chemical approach to predicting the thermal expansion of compounds in the NZP family, Inorg. Mater. 39 (10) (2003) 1013–1023.

[4] D.K. Agrawal, C-Y. Huang, H.A. McKinstry, NZP: a new family of low-thermal expansion materials, Int. J. Thermophys. 12 (4) (1991) 697–710.

[5] M.V. Sukhanov, M.M. Ermilova, N.V. Orekhova, V.I. Petkov, G.F. Tereshchenko, Catalytic properties of zirconium phosphate and double phosphates of zirconium and alkali metals with a $NaZr_2(PO_4)_3$ (NZP) structure, Russ. J. Appl. Chem. 79 (4) (2006) 614–618.

[6] W. Miller, C.W. Smith, D.S. Mackenzie, K.E. Evans, Negative thermal expansion: a review, J. Mater. Sci. 44 (2009) 5441–5451.

[7] E.J. Liang, Negative thermal expansion materials and their applications: a survey of recent patents, Rec. Pat. Mater. Sci. 3 (2010) 106–128.

[8] V.I. Petkov, M.V. Sukhanov, M.M. Ermilova, N.V. Orekhova, G.F. Tereshchenko, Development and synthesis of bulk and membrane catalysts based on framework phosphates and molybdates, Russ. J. Appl. Chem. 83 (10) (2010) 1731–1741.

[9] L.O. Hagman, P. Kierkegaard, The crystal structure of $NaM_{e2}{}^{IV}(PO_4)_3$, $M_{e2}{}^{IV}$ = Ge, Ti, Zr, Acta Chem. Scand. 22 (1968) 1822–1832.

[10] R. Roy, E.R. Vance, J. Alamo, [NZP], a new radiophase for ceramic nuclear waste forms, Mater. Res. Bull. 17 (5) (1982) 585–589.

[11] H.S. Park, I.T. Kim, H.Y. Kim, S.K. Ryu, J.H. Kim, Immobilization of molten salt waste into $MZr_2(PO_4)_3$(M = Li, Na, Cs, Sr), J. Radioanal. Nucl. Chem. 268 (3) (2006) 617–626.

[12] J. Brown, D. Hirschfeld, D.M. Liu, Y.P. Yang, T.K. Li, R.R. Swanson, R.E. Aken, J.M. Kin, Ceramic materials with low thermal conductivity and low coefficients of thermal expansion, US Patent, No.102836 (1992).

[13] S.Y. Limaye, D.K. Agrawal, H.A. Mckinstry, Synthesis and thermal expansion of $MZr_4P_6O_{24}$ (M = Mg, Ca, Sr, Ba), J. Am. Ceram. Soc. 70 (10) (1987) 232–236.

[14] K.V. Govindan Kutty, R. Asuvathraman, R. Sridharan, Thermal expansion studies on the sodium zirconium phosphate family of compounds $A_{1/2}M_2(PO_4)_3$: effect of interstitial and framework cations, J. Mater. Sci. 33 (1998) 4007–4013.

[15] J. Alamo, J.L. Rodrigo, High temperature neutron diffraction study of $CaZr_4(PO_4)_6$, Solid State Ionics 63–65 (1993) 678–683.

[16] C. Rashmi, O.P. Shrivastava, Synthesis and crystal structure of nanocrystalline phase: $Ca_{1-x}M_xZr_4P_6O_{24}$ (M = Sr, Ba and x = 0.0–1.0), Solid State Sci. 13 (2011) 444–454.

[17] S.Y. Limaye, D.K. Agrawal, H.A. McKinstry, R. Roy, Low expansion ceramic, US Patent, No. 4801566 (1989).

[18] D.K. Agrawal, V.S. Stubican, Synthesis and sintering of $Ca_{0.5}Zr_2P_3O_{12}$ - a low thermal expansion material, Mater. Res. Bull. 20 (1985) 99–106.

[19] N. Chakraborty, D. Basu, W. Fischer, Thermal expansion of $Ca_{1-x}Sr_xZr_4(PO_4)_6$ ceramics, J. Eur. Ceram. Soc. 25 (2005) 1885–1893.

[20] C.S. Yoon, J.H. Kim, C.K. Kim, K.S. Hong, Synthesis of low thermal expansion ceramics based on $CaZr(PO_4)_6$–Li_2O system, Mater. Sci. Eng. B79 (1) (2001) 6–10.

[21] E.J. Liang, Y. Liang, Y. Zhao, J. Liu, Y.J. Jiang, Low-frequency phonon modes and negative thermal expansion in $A(MO_4)_2$ (A = Zr, Hf and M = W, Mo) by Raman and Terahertz Time-Domain Spectroscopy, J. Phys. Chem. A 112 (49) (2008) 12582–12587.

[22] V.S. Kurazhkovskaya, D.M. Bykov, E.Y. Borovikova, N.Y. Boldyrev, L. Mikhalitsyn, A.I. Orlova, Vibrational spectra and factor group analysis of lanthanide and zirconium phosphates $M^{III}{}_{0.33}Zr_3(PO_4)_3$, where M^{III} = Y, La–Lu, Vib. Spectrosc. 52 (2010) 137–143.